Detection and Extraction of Buildings from Interferometric SAR Data

P. Gamba, *Member, IEEE*, B. Houshmand, *Member, IEEE*, and M. Saccani

Abstract— **In this paper we present a complete procedure for the extraction and characterization of building structures starting from the three-dimensional (terrain elevation) data provided by interferometric SAR measurements. Each building is detected and isolated from the surroundings by means of a suitably modified machine vision approach, originally developed for range image segmentation. The procedure is based on a local approximation of the 3D data by means of best-fitting planes. In this way, a building footprint, height and position, as well as its description with a simple 3D model, are recovered by a self-consistent partitioning of the topographic surface reconstructed from interferometric radar data.**

The method is validated by the analysis of 10 m resolution data recorded over Santa Monica, Los Angeles, by the airborne TOPSAR system operated by NASA-JPL. We present good results with respect to the detection of commercial buildings, and a quantitative evaluation shows that the heights of these structures are recovered almost with the same precision as the original data. Larger errors are instead evidenced in their footprints.

Keywords—**SAR urban analysis, 3D building extraction.**

I. Introduction

The urban environments, with their complex structure composed of buildings of different kinds and shapes, small and/or large green areas, infrastructures (roads, railroads, bridges, ...) and continuously changing suburbs have constantly been a challenge for remote sensing analysts. Notwithstanding the large number of works on the interpretation of urban images acquired by different sensors, from the *classic* photocameras to Synthetic Aperture Radars (SAR) ([1], [2]) from multispectral [3] to hyperspectral sensors (like AVIRIS [4]), a large amount of information is still hidden in the raw data.

On the other hand, with the largest part of the population in the world already settled in towns and cities, it is increasingly important to develop a set of flexible tools for the analysis, monitoring and planning of urban environments. Even the study of geological and hydrological risks in urban areas can give useful hints to prevent and alleviate hazards like earthquakes and floods, whose costs (in terms of lives more than dollars) have been steadily increasing in the past years [5].

To this aim, the continuous trend in research is to merge measurements and data from different sensors [6]-[8] to refine, by means of this interaction, the quality of the information extracted. Contemporarily, very interesting analyses in recent years have been dedicated to investigate how all-weather sensors, like the SAR, can be exploited to evaluate bio- and geophysical parameters in urban areas [9]. In particular, many papers have been presented aiming at determining which radar data (in terms of polarization [10], [11], wavelength [12], [13] or viewing angle [14], [15]) are more useful for urban image analysis.

However, very few papers are devoted to the use of Interferometric SAR (IFSAR) measurements ([16], [17]) for urban image analysis: one of them is [4], where IFSAR and AVIRIS data are merged to better distinguish buildings from green areas. Indeed, the 3D measurements obtained by this system may be extremely useful for extracting the complete topography of a urban environment (for instance, for hydrological purposes) as well as for gathering more insight on particular structures or infrastructures (like the road network).

Analysis of the IFSAR terrain elevation data in urban areas are difficult due to the insufficient spatial resolution (with respect to urban features), multiple scattering due to the building geometries, and layover effects, in addition to the intrinsic IFSAR system level noise. Therefore, it is clear that there is still a strong need to evaluate which type of information is available from these data and to what extent it is possible to extract them.

The resolution problem is being increasingly resolved by the new generation of radar sensors that are currently operational or will be operational in the near future, like the NASA/JPL AIRSAR system [18]-[20] (currently a 40 MHz system, but to get upgraded to 80 MHz) and the DLR E-SAR system [21]. The goal of these systems is to provide a 1-meter level spatial resolution, which therefore can resolve many of the objects present in an urban environment. As for the second problem, instead, we found very interesting to apply to the original remote sensing images some suitable machine vision approaches. Indeed, even if developed for very different situations, these procedures are of invaluable utility when used in this context.

In this work we focus on the task to extract information on urban structures of interest from high resolution IFSAR data. Specifically, we want to automate the detection (and subsequent analysis) of the height and shape of the buildings present in a given area. To this aim, we apply to the original data a segmentation algorithm able to exploit their resolution, while maintaining at the same time a high robustness to noise.

The paper is organized as follows: Section II presents the complete building detection strategy used in the 3D image analysis procedure. Section III, instead, shows the results obtained on actual images and discusses their significance for urban area analysis as well as their limit for a

P. Gamba and M. Saccani are with Dipartimento di Elettronica, Università di Pavia, Via Ferrata, 1, I-27100 Pavia, Italy, while B. Houshmand is with Jet Propulsion Laboratory, 800 Oak Grove Drive, Pasadena, CA

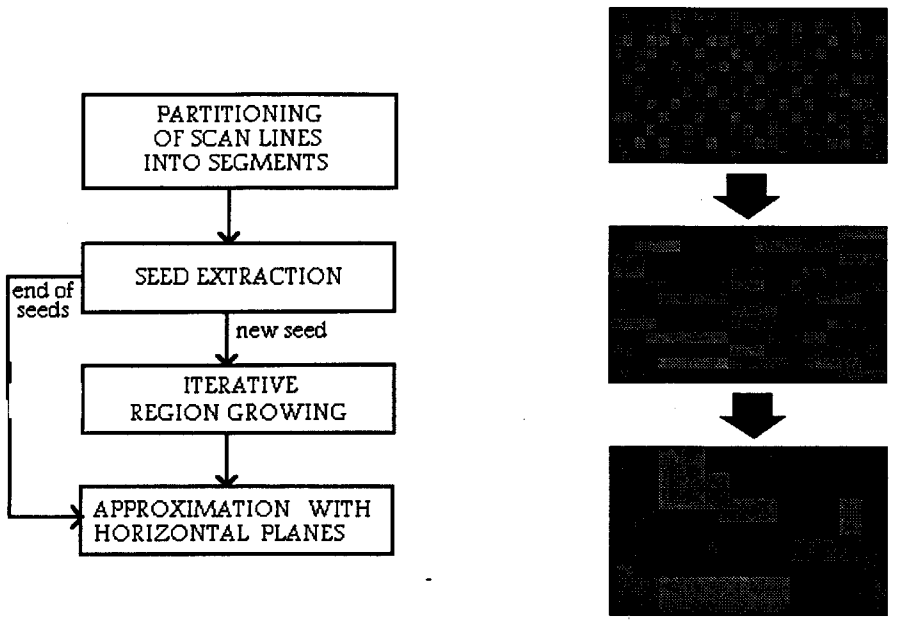

Fig. 1. The block diagram of the segmentation algorithm used to analyze the IFSAR images.

more refined model-based extraction of the urban profile. Finally, in section IV some conclusions and lines of thought for future improvements are introduced.

II. Building Detection Strategy

Our goal is to extract the significant buildings from interferometric SAR images, that is to locate some *special regions* inside them. Therefore, we must face a segmentation of the image, since segmenting an image means to divide it into meaningful objects according to a given criterion. The task is analyzed in [22], where some heuristic criteria for the correction of the shape of isolated buildings are applied to interferometric data, and in [23], where the author explored, in a more general context, how to find the parameters of a given building model that best fit the measured 3D data. Both papers, however, do not address the problem of building extraction in a crowded, complex urban environment.

On the other hand, we may find useful to rely on consolidated approaches studied in machine vision. In this field, when considering 3D (usually called *range*) images, generally the criteria applied to segment the data are geometric ones (see for instance [24] or [25]), often involving the principle of plane-fitting (i.e. to find the plane which better approximates a given surface). In our situation this approach can be useful when looking for the regions corresponding to the building roofs. The idea is therefore not only to partition the image (each pixel must belong to one region) but also to discard the data that do not carry useful information during image segmentation.

To this aim, the simplest possible algorithm could be an iterative region growing approach: we start from randomly chosen pixels (*seeds*) and examine all the adjacent ones. If one of them is *sufficiently* near to the seed in the 3D space (where *sufficiently* must be defined by a suitable threshold), it is added. However, this is the only a first step of the segmentation, since the data is now divided into regions whose geometric characteristics are still to be determined (for instance, are they planes or not?). However, since we expect that almost all of the structures in a urban environments can be roughly described by polyhedra with plain faces, we can try to approximate each of these regions by a plane.

This idea can be further improved by the algorithm outlined in [26]. In this approach the primitives of segmentation are not pixels, but scan lines (the lines of the image), in order to save cpu time. Grouping lines, it's faster to find consistent planes hidden in noisy data. We applied this procedure, suitably changed, following three processing steps (see also fig. 1).

First step: scan line segmentation. The pixels belonging to the same scan line are grouped into segments according to a simple geometric criterion [27]: a curve is iteratively broken in two parts until no point of the original curve is far from the resulting segment chain more than a given threshold (θ_1). Since one scan line of the IFSAR image can be viewed as a curve in the third (*range*) dimension, this step represent an approximation by segments of the 3D topographic data along each line of the image. Moreover, since this 3D curve actually presents some discontinuities (the building edges, for instance), we follow [26] in using edge pixels (pixels with value very different from their left or right neighbour) as further breakpoints. Finally, each segment found is recorded in a list, with pointers to its neighbors (i.e. adjacent segments).

Second step: planar region aggregation. It consists of finding first the *seeds* for the aggregation and then to perform a region growing procedure to get the final, segmented

image. Each seed is constituted by three adjacent segments (longer than a given threshold θ_2) belonging to different scan lines. The seeds are ordered and used for segment aggregation into planar surfaces starting from the one nearest to the ideal condition of three segments aligned on a plane. This condition is measured by controlling that the directions and the intercepts of the seed segments coincide as much as possible (see also [26], eq. (11)). The index used is

$$i_p = 0.5 + \frac{1}{12}\left(\sum_{i \neq j} \frac{m_i \cdot m_j}{|m_i|\,|m_j|} + \frac{n_i \cdot n_j}{|n_i|\,|n_j|}\right) \qquad (1)$$

where $m_i = (a_i, -1)$, $n_i = (b_i^*, -1)$, and $s_i = a_i x + b_i$, $i = 1, 2, 3$ are the algebraic expressions of the segments of a seed.

Next, the iterative region growing is performed. All the segments adjacent to the best seed are examined: if a segment is close enough (again, by a threshold θ_3) with respect to both its ends to the plane that approximates the seeds, it is added to the region. This process is iterated (considering the new region as an enlarged seed), until no more expansion is possible. Successively, less optimal seeds are used for the same process until the image is divided into planes and only segments that could not be aggregated are left.

Third step: the final refinement. The previous segmentation may be improved by means of heuristic algorithms or more refined edge detection scheme to adjust the boundaries of the regions. In [26] the simple method to re-assign boundary pixels to the nearest plane is suggested.

As already stated above, to this procedure we must add a last step requiring that the best-fitting plane for each region is approximated with an horizontal one, for a first, imprecise simulation of building roofs.

Moreover, we must note that not all the pixels of the original image belong to a plane, when the algorithm stops: points affected by large noise, or regions where no actual planar surface is observable (for instance, trees in a park) are not aggregated. These points could be due to an error to be corrected or could carry important information not to be missed. At this point of the procedure it is difficult to say which is the case, until no further information is gained.

A. *Critical points of the algorithm for interferometric data segmentation*

It is clear that the method described in the preceding paragraphs was developed originally as a machine vision approach to range image segmentation. Therefore, several problems arise when we try to obtain significant results from the application of this algorithm to the topographic data computed by SAR interferometry. We discuss here first the choice of the thresholds in the above outlined procedure ($\theta_1 - \theta_3$), and then the point of pre-filtering or not the original data. Finally, a few words will be also dedicated to the choice to approximate each plane with an horizontal one in the final resulting 3D topography.

We found that, as far as the first step (scan line partitioning) is concerned, the breakpoints based on the original algorithm were not always the optimal ones. In low resolution SAR images, it is necessary to overpartition the lines because of the small number of points defining each structure, while a different choice causes the merging of separate buildings into a unified object. It can be argued that this method introduces some kind of error in the segmentation procedure. However, the problem is later corrected by the segment grouping carried out in the growing process (while an underpartitioning would have been impossible to adjust). In a few words, this correspond to a choice of θ_1 (see the previous paragraph) as low as $0.8\sigma_{img}$ where σ_{img} is the mean local image variance of the original data.

For the same reason also the definition of *edge pixels* may be changed according to the type of building that we want to extract. For instance, for high structures, edges correspond to large height steps, while when looking for residential objects, we have lower values. In this research we adopted a sort of conceptually pyramidal approach, and started by first extracting the large buildings. When working instead on residential structures we think that it would be better to lower the value of what is to be considered an edge accordingly.

The second threshold in the algorithm (θ_2) is set to evaluate only significant segments when looking for plane *seeds*. It is clear that, to discard possible error, it must be chosen as small as possible with respect to the physical characteristics of the searched objects and the resolution of the image. As for our IFSAR data are concerned (10 m resolution, 5 m posting), even segments of two of three pixels are meaningful since there exist buildings with these dimensions. This requires to consider a large number of seeds, leaving to a successive interpretation step the task to choose if all the planar regions are meaningful or not. Therefore a value smaller than the original value of 10 is used.

Finally, the last parameter to be tuned (θ_3) defines somehow which is the largest difference between a plane and a given segment to allow its aggregation. This parameter refers to the distance between the plane and the segment ends. Therefore, even if in [26] it is suggested a unique value for any situation, it is intuitive that longer segments require lower values (they can be aggregated only if they are significantly consistent with those already grouped), while smaller ones can be considered also in worse cases. We found, however, that the overpartitioning rule in the first step of the procedure usually provide only small segments, and the choice of a varying θ_3 does not change the quality of the results.

An other important point regards the pre-filtering of the data. We decided not to make any pre-filtering of the image (even if this could be extremely critical for the image analysis) because classical approaches to SAR filtering (see [28] for a recent review) usually provide also a smoothing of the image, that would have caused a loss of resolution, making the identification of the correct borders of each building difficult. Instead, the range segmentation offers a self-consistent smoothing of the 3D data driven by the

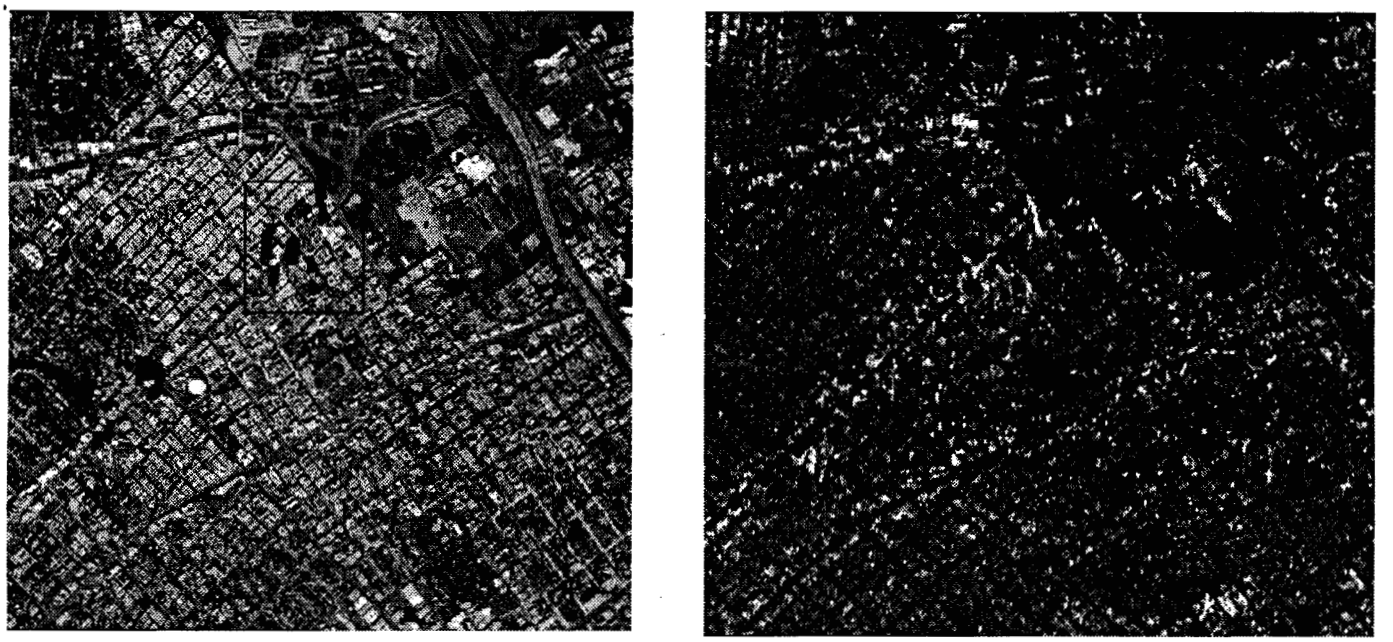

Fig. 2. On the right, an AIRSAR C-band image of Santa Monica, West Los Angeles (VV polarization). For a visual comparison, on the left an aerial photo of the same area is displayed. The blocks of black pixels correspond to large building shadows in the photograph, and to pixels labeled as "erroneous acquisition" in the SAR data.

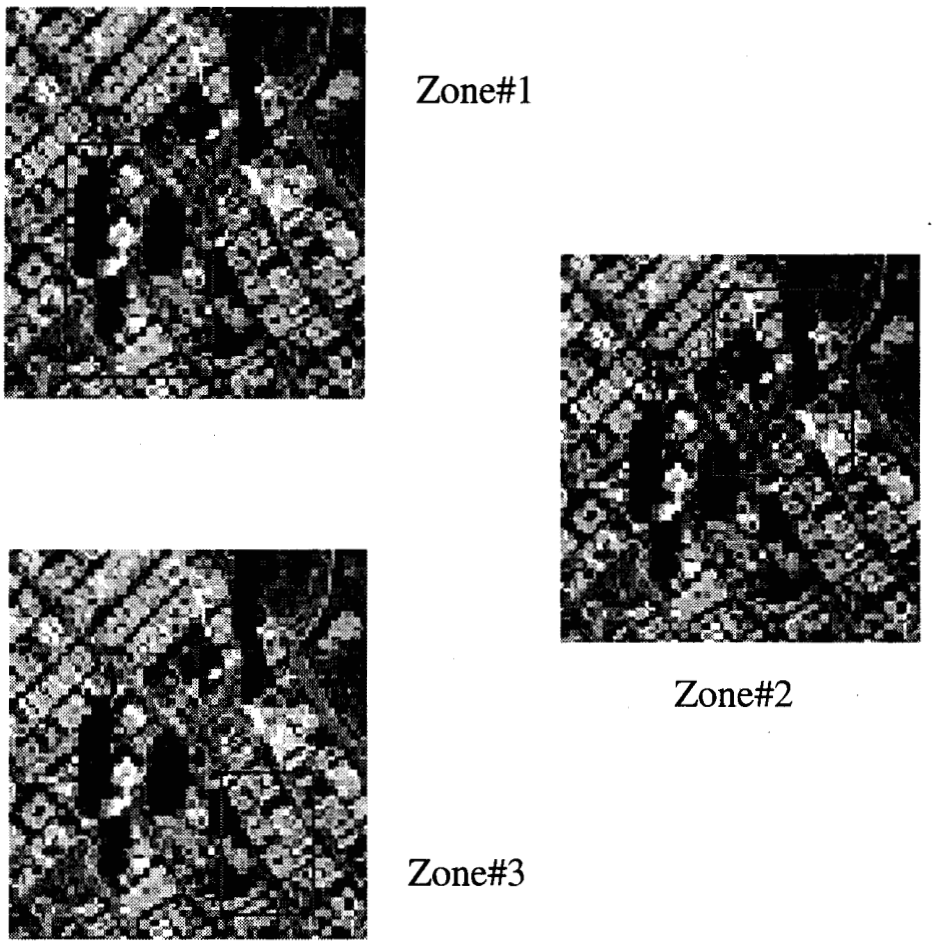

Fig. 3. Zoomed views of the aerial image in fig. 2 showing the three zones around Wilshire Boulevard that were analyzed in this paper.

simple building models (essentially, parallelepipeds) that we use. In other words, the best-fitting plane procedure above delineated can be seen as the application of the *optimum filter* to the problem to recover a *signal* corrupted by noise knowing its shape (again, it's a plane). For this reason there is no need to perform any prefiltering. It is true, however, that more recent papers have developed pyramidal [29] or filter bank approaches [30] to avoid as much as possible the degradation of SAR image details after denoising. These methods allow a more precise edge location in radar measurements affected by noise, and we plan to add some sort of edge analysis as a further information source useful for our task.

Finally, we want to add a practical note: the approximation of the range regions with horizontal planes is made by using the mean value between the points belonging to each slanting plane. This introduces a further approximation which affects the values of the heights of the the buildings. On the other hand it minimizes evaluation errors due to noise and/or false reflections.

III. Experimental Results and Discussion

The interferometric SAR range image used to show the results of this research covers a portion of Santa Monica, in the metropolitan area of Los Angeles (see fig. 2). It is a range image, that is to say an array of numbers representing the surface elevation with respect to a reference plane. So, this image already gives us the three-dimensional profile of the urban surface.

The data were obtained with an interferometric SAR, the AIRSAR system, operated by NASA/JPL and mounted on a DC8 plane. The system is operated at C-band (5.6689 cm wavelength) with a 40 Mhz pulse bandwidth, and has a nominal height accuracy in the order of $\pm$ 2.5 m. The spatial resolution of the SAR system is therefore 3.75 meters in range direction but, after the interferometric processing by phase unwrapping procedures [31], [32], this range is reduced to 7.5 meters, since two pixels are averaged. The averaging in the azimuth direction is also performed to yield a square resolution cell. So, the ground range resolution for the mid-swath area (nominally 45 radar incident direction) is about 10 meters, even if the images of the AIRSAR interferometric elevation data are provided after sampling at 5 meter postings, geocoded and rectified.

This resolution makes the building detection an extremely difficult task; anyway, these data were used in this research just to show how well the procedure behaves even when the spatial coarseness of the measurements is relatively low (10 m are comparable with most of the building footprints' dimensions).

The images we show here come from a larger data series recorded on August 5, 1994, from the height of 11,000 meters. The flight path was from 33.97 N latitude, -118.47 longitude to 33.97 N latitude, -118.41 longitude. The radar look angle for the proposed area is nominally 45° and shadow/layover effects are observable as it can be seen by looking at the black pixels in fig. 3 left, corresponding to incorrect measurements that were discarded by the TOPSAR data processor.

We stress that we present here only a very small part of the data recorded.

A. Wilshire Boulevard

Within the study area, we applied the above outlined procedure to a subimage covering part of Wilshire Boulevard (East Santa Monica). The image was in turn divided into three parts (see fig. 3) for a better analysis, and the above presented algorithm was applied separately to each of them. This was done in order to handle the data easily and to facilitate the identification of the buildings.

However, it should be mentioned that the original 3D data lack the definition of a suitable ground level, because multiple reflections at the building edges produce responses that alter this value. To overcome this problem, we used the same procedure discussed in [4] and compute the overall height distribution of the data. Ground level is taken as the highest peak in the hystogram, due to the presence in the area of large flat green areas, and points that have lower values are discarded. By means of this technique, only a very small number of pixels (in our area, less than 2%, and mainly around building edges) are not considered, but the successive detection procedure is considerably improved.

The results of the complete analysis for zone # 1 of fig. 3 are shown in fig. 4: the upper picture represents the raw 3D surface extracted from the interferometric measurements, while the other one shows the output of our program. It is immediately clear that the raw data are confusing, with disturbing noise and blurred building edges, while in the 3D graph obtained from our algorithm the profiles of the most relevant buildings are now evident. Moreover, each of them is now a separate object. In other words, we operate simultaneously on fig. 4(a) three operations:

1. a denoising procedure, as it is clear for instance looking at the roofs of the building in fig. 4(b);
2. a structure recognition, because now we are able to distinguish the buildings from their (probably less interesting) surroundings;
3. an image segmentation.

As a final comment, we should note that there are also some artifacts still visible for the lower objects present in the scene, that we neglect for the moment.

More in detail, in fig. 5 and 6 two of the buildings situated in Wilshire Boulevard are shown by simply retaining only those 3D values that we found belonging to each of them. After that, their shape was compared either with maps or to the information that we extracted from a color image of the analyzed zone co-registered with the IFSAR original data. Furthermore, we had a number of color photographs taken on the ground depicting the main buildings of Wilshire Boulevard. The photographs allowed us to identify each building and to have a first idea of the validity of our results by means of a rough comparison of its shape and height. These figures show, respectively, the reconstructed shapes of the Coastal Federal Bank and 1755 Wilshire Boulevard, together with some photographs from the ground.

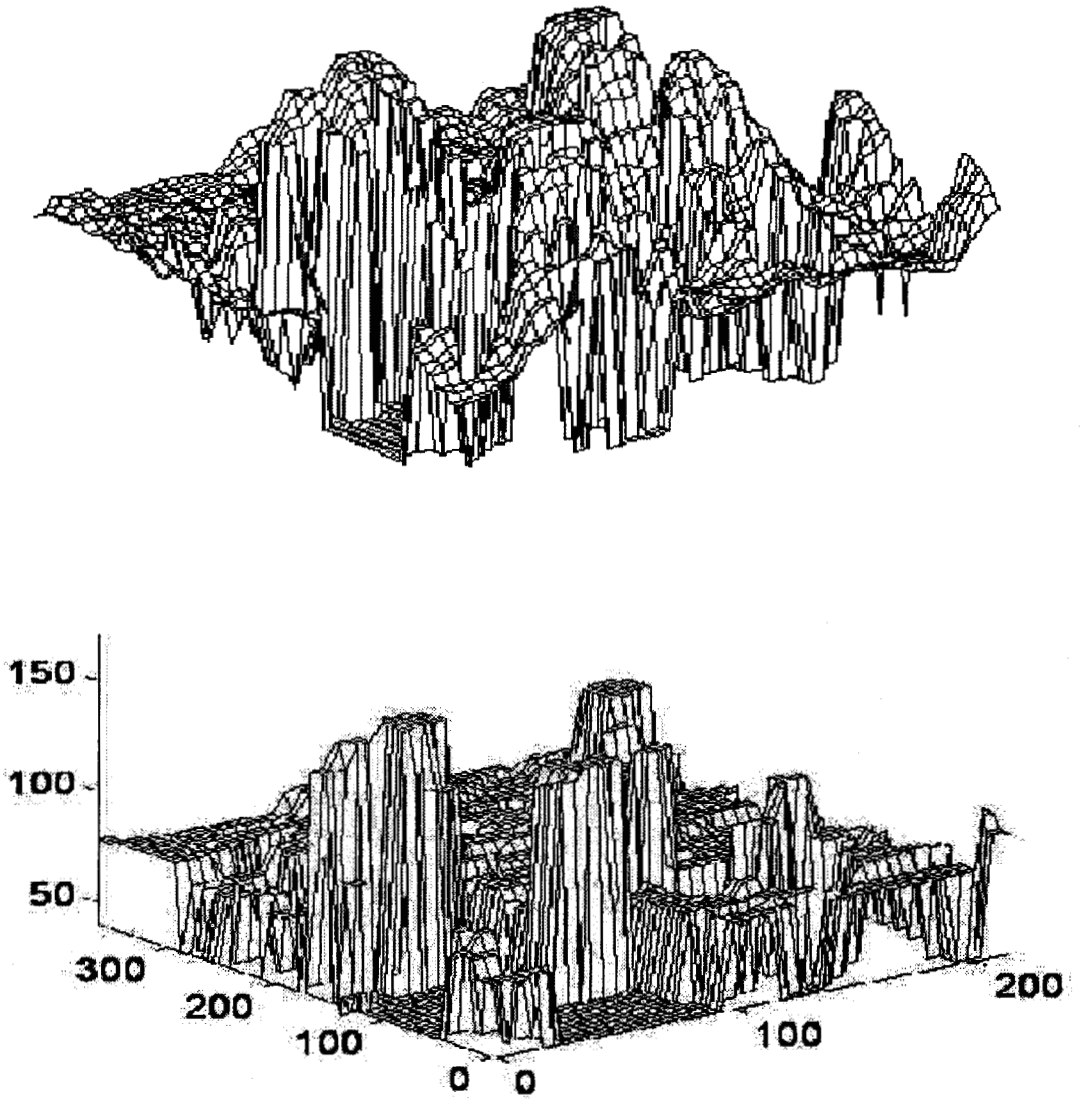

Fig. 4. The raw three-dimensional interferometric data provided by the TOPSAR system above the first zone of fig. 3 and the reconstructed building profiles after the data analysis.

B. Some comments on the results

The first important thing to observe is that all the large buildings portrayed in the photographs had been extracted by our algorithm without any exception, and this is the minimum results we expected for. In addition, we observe that all the extracted structures correspond to commercial, financial and directional sites, that is buildings characterized by relevant heights and large dimensions. Smaller houses on the contrary are much more difficult to distinguish because of their small dimension. Moreover, we have not yet collected ground truth in a sufficient detail for that area to help in tuning the parameters of the extraction procedure. Finally, IFSAR data with higher spatial resolution than the one we used are needed to extract and recognize them; to this aim, the 2.5 m resolution measurements, that the new TOPSAR system will be able to provide, may give sufficient information for a more detailed extraction of the less evident structures.

Each building carries at least three types of information, namely its position, shape and height. As far as the positions of the buildings are concerned, comparing our output graph with the color image, we have noticed that they are substantially correct (within the range of spatial precision of the data).

Instead, fig. 7 shows the footprints of all the largest buildings in the three zones of fig. 3, and a comparison with their actual shape is performed. It is clear that while the reconstructed shape of the objects is generally a sufficiently good representation of the real one, the area of the buildings is heavily underestimated. The main reason is the shadowing/overlay effect due to the relative position of the airplane carrying the radar and the illuminated large bodies on the ground. It affects the accuracy of the 3D

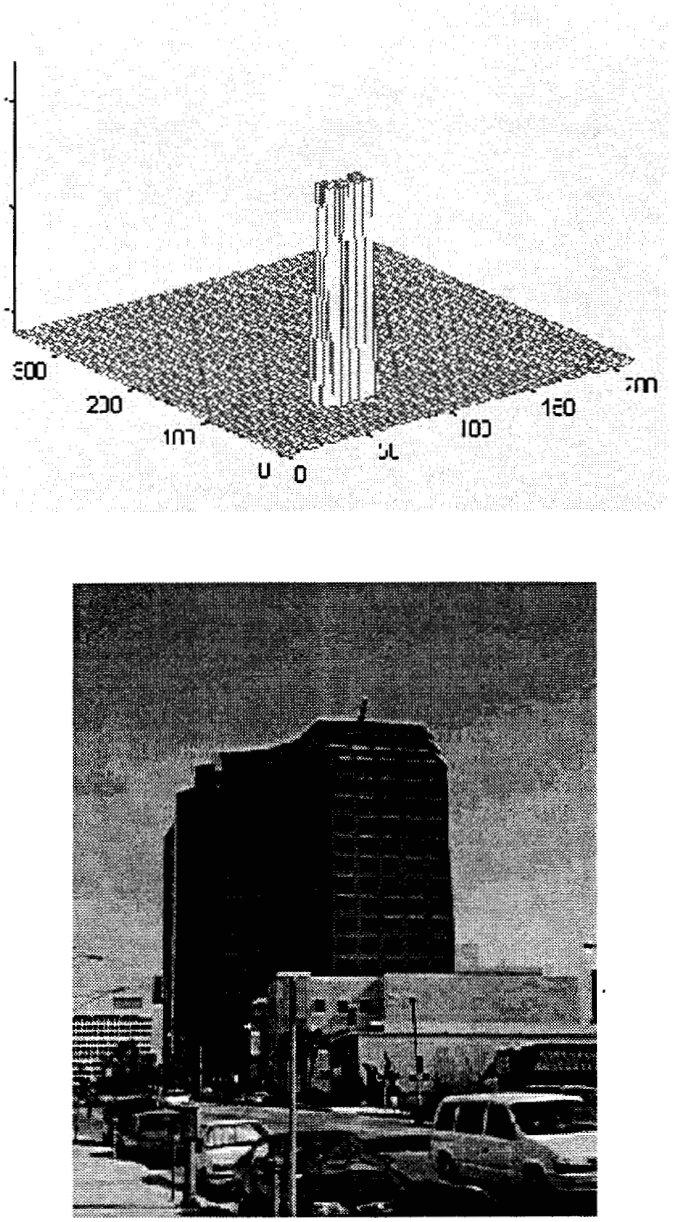

Fig. 5. The Coastal Federal Bank in Wilshire Boulevard: the building profile as reconstructed from IFSAR data and a photo from the ground.

data related to the transition between a building and the road (or another building, the grass, etc.). As a result, it is hard for the algorithm to find good borders, and this was the reason to obtain a building footprint mask using another sensor in [4]. Table I presents the errors computed as a percentage of the original area for the same examples of fig. 7. Worse results are related to buildings "badly" oriented with reference to the flight direction (this is the case, for instance, of the Barrington Plaza Apt.)

To overcome the problem, we introduced a further refinement step to our procedure, devoted to two tasks: reduce the unclassied pixels, and merge horizontal planes that have very similar heights. The first task is due to the fact that in our final images there are many pixels not belonging to any plane; they are added to the nearest classified set if it is sufficiently near (less than 3 times the SAR precision, i. e. $\pm$ 7.5 m). Moreover, since the previous results show that probably each building roof is detected as a set of differently oriented planes (due to SAR processing errors, or to spurious reflections) we merged the final detected surfaces that are adjacent and very similar in height (the threshold is the same than above). Heights are changed taking into account the weight (in terms of pixels) of each merged set. The results obtained with the aid of this technique are presented in Table I, and show a significant improvement in the footprint estimate in almost all the cases.

The last comment regards the building heights, that happen to be necessarily approximated because we model each structure by using only planar surfaces; moreover, all the roofs are taken as flat ones. Nevertheless, the resulting values seem to be in very good accordance with those deter-

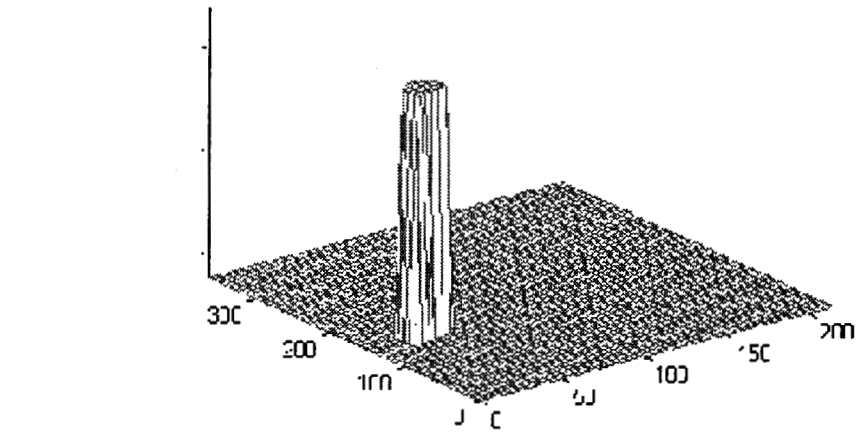

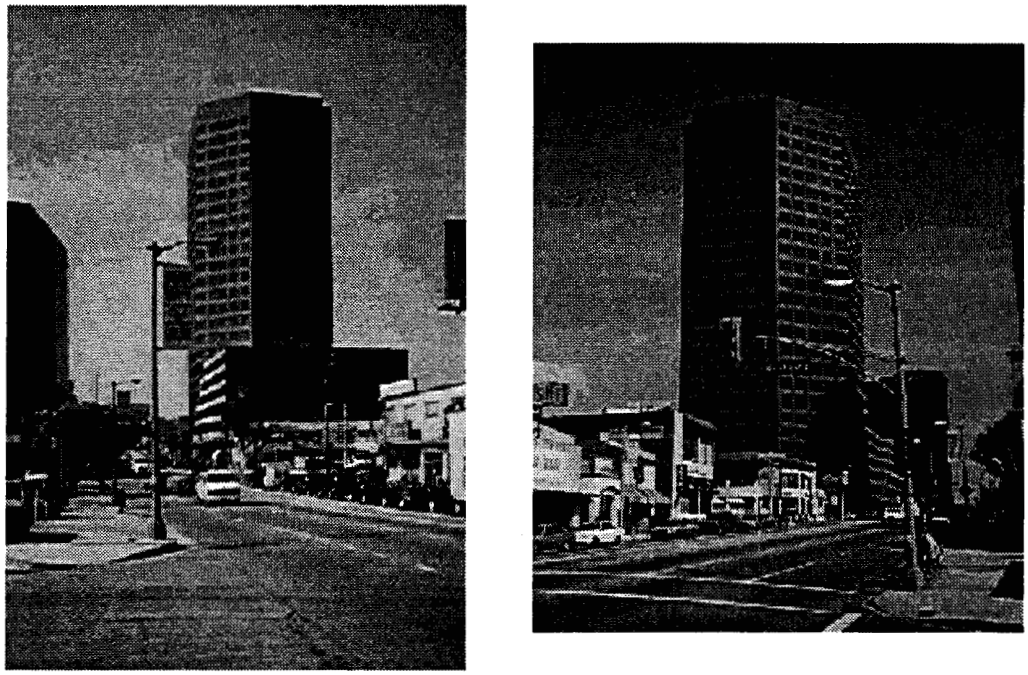

Fig. 6. 11755 Wilshire Boulevard: the building profile as reconstructed from IFSAR data and two photos from the ground.

mined from field measurements. Table II shows the differences between the extracted heights and the actual values, together with the mean error; again, the minus sign represents an underestimate. This result (±4.9 m) must be compared with the mean error that we expect (according to [20]) from TOPSAR measurements, i. e. ±2.5 m. We may say that the loss in resolution from the original data to the classified one is limited, especially considering that this result is partially due to the error in the location of the ground level. Moreover, we think that it is better in an urban environment to have less precise information on each built structure as a single entity than to know the exact 3D position of each measured point, without knowing to what it belongs. In other word, we believe that the limited loss in precision of our results with respect to the original data is more than compensated by the recognition of interesting urban structures.

IV. Conclusions

This work presents the application of a modified machine vision approach to 3D data extracted from interferometric SAR measurements. The proposed approach has proved to be useful in reconstructing the 3D structure of large commercial structures from a 10 m resolution data. Their shape is sufficiently well reconstructed and their height is found with an absolute mean precision around 2 m and standard deviation of ±4.9 m. However, building footprints are largely underestimated.

Therefore, the proposed approach exploits almost completely the vertical (±2.5 m) resolution of the original data and enables us to recognize and isolate those buildings that raise well over their surroundings, but lacks a suitable system to overcome layover/shadowing effects. A further refinement of this work is also needed for the recognition and

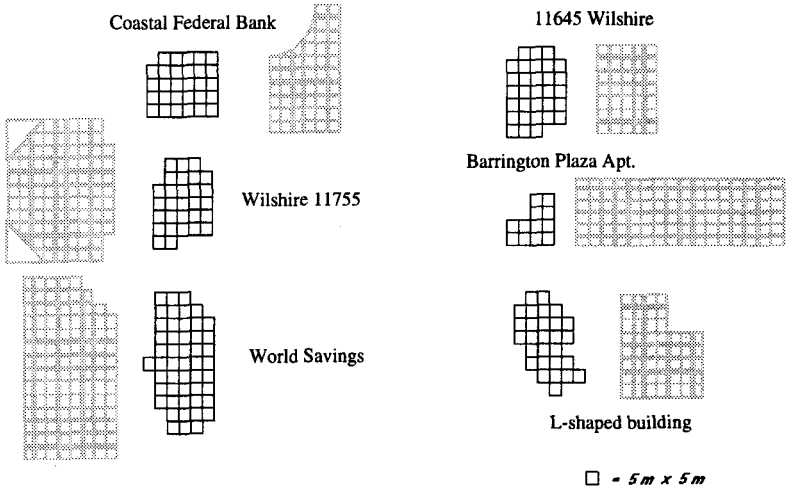

Fig. 7. The footprints of all the buildings extracted from the three subimages in fig. 3 compared with their actual sections (shadowed): a square corresponds to 25 mq.

analysis of smaller buildings such as residential houses by using both more detailed data and improved extraction algorithms.

However, even these preliminary results show that there is a strong possibility to extract from IFASR data building models characterized with a precision only slightly worse than the original topographic data. Such an analysis could be extremely useful for research as well as possible commercial applications, like "on line" detection of the 3D characteristics of real estates.

REFERENCES

[1] F.M. Henderson and Z.G. Xia, "SAR applications in human settlement detection, population estimation and urban land use pattern analysis: a status report," *IEEE Trans. on Geoscience and Remote Sensing*, Vol. 35, No. 1, pp. 79-85, 1997.

[2] Z.G. Xia, "Applications of multi-frequency, multi-polarization and multi-incident angle SAR systems in urban land use and land cover mapping," Proc. of *IGARSS'96*, Vol. IV, pp. 2310-2314, Lincoln, Nebraska, July 1996.

[3] J. Hrikkonen, I. Kanellopoulos, A. Varfis, A. Steel and K. Fullerton, "urban land-use mapping with multi-spectral and SAR satellite data using neural networks," Proc. of *IGARSS'97*, Vol. IV, pp. 1660-1662, Singapore, Aug. 1997.

[4] G.F. Hepner, B. Houshmand, I. Kulikov, and N. Bryant, "Investigation of the potential for the integration of AVIRIS and IFSAR for urban analysis," *Photogrammetric Eng. Remote Sensing*. Vol. 64, No. 8, pp. 512-520,1998.

[5] G. Bertz, A. Smolka, "Urban earthquake loss potential: economical insurance aspects," Proc. of *10th European Conf. on Earthquake Engineering*

[6] B.N. Haack, "Multisensor data analysis of urban environments," *Photogrammetric Eng. Remote Sensing*, Vol. 50, No. 10, pp. 1471-1477, 1984.

[7] D.J. Weydahl, X. Becquey, T. Tollefsen, "Combining ERS-1 SAR with optical satellite data over urban areas," Proc. of *IGARSS'95*, Vol. IV, pp. 2161-2163, Florence, Italy, Sept. 1995.

[8] M. Caetano, J. Santos, A. Navarro, "A multi-strategic approach for land use mappings of urban areas by integrating satellite and ancillary data," Proc. of *IGARSS'97*, Vol. I, pp. 240-242, Singapore, Aug. 1997.

[9] Z.G. Xia and F.M. Henderson, "Understanding the relationships between radar response patterns and the bio- and geophysical parameters of urban areas," *IEEE Trans. on Geoscience and Remote Sensing*, Vol. 35, No. 1, pp. 93-101, 1997.

[10] M.L. Bryan, "Analysis of two Seasat Synthetic Aperture Radar images of an urban scene," *Photogrammetric Eng. Remote Sensing*, Vol. 48, No. 3, pp. 393-398, 1982.

[11] Y. Dong, B.C. Foster, C. Ticehurst "Decomposition of radar signatures from built and natural targets," *International Archives of Photo. and Remote Sensing*, Vol. XXXI, part B7, pp. 196-203, 1996.

[12] F.M. Henderson, "An evaluation of seasat SAR imagery for urban analysis," *Remote Sensing of Environment*, Vol. 12, pp. 439-461, 1982.

[13] B.N. Haack, "L- and X-band like- and cross-polarized Synthetic Aperture Radar for investigating urban environments," *Photogrammetric Eng. Remote Sensing*, Vol. 50, No. 3, pp. 331-340, 1984.

[14] B. Dousset, "Synthetic Aperture Radar imaging of urban surfaces: a case study," Proc. of *IGARSS'95*, Vol. IV, pp. 2092-2096, Florence, Italy, Aug. 1995.

[15] D.J. Weydahl, "Identifying urban features using RADARSAT images taken at multiple incidence angles," Proc. of *IGARSS'97*, Vol. I, pp. 287-289, Singapore, Aug 1997.

[16] E. Rodriguez, J.M. Martin, "Theory and design of interferometric synthetic aperture radars," *IEE Proc. on Radar, Sonar and Navigation*, Vol. 139, No. 2, pp. 147-159, 1992.

[17] R. Gens and J.L. Van Genderen, "SAR Interferometry: issues, techniques, applications," *International Journal of Remote Sensing*, Vol. 17, pp. 1803-1835, 1996.

[18] H.A. Zebker, S.N. Madsen, J.M. Martin, K.B. Wheeler, T. Miller, Y. Lou, G. Alberti, S. Vetrella, A. Cucci, "The TOPSAR interferometric radar orographic mapping instrument," *IEEE Trans. on Geoscience and Remote Sensing*, Vol. 30, No. 5, pp. 933-940, 1992.

[19] S.N. Madsen, H.A. Zebker, J.M. Martin, "Topographic mapping using radar interferometry: processing techniques," *IEEE Transactions on Geoscience and Remote Sensing*, Vol. 31, No. 1, pp. 246-256, 1993.

[20] S.N. Madsen, J.M. Martin, H.A. Zebker, "Analysis and evaluation of the NASA/JPL TOPSAR across-track interferometric SAR system," *IEEE Trans. on Geoscience and Remote Sensing*, Vol. 33, No. 2, pp. 383-391, 1995.

[21] M. Coltelli, G. Fornaro, G. Franceschetti, R. Lanari, A. Moreira, E. Sansoti, R. Scheiber, M. Tesauro, T.I Stein, "Results of the Mt. Etna interferometric E-SAR campaign," Proc. of *IGARSS'97*, Vol. IV, pp. 1554-1556, Singapore, Aug. 1997.

[22] G.R.Burkhart, Z. Bergen, R. Carande, W. Hensley, D. Bickel, J.R. Fellerhoff, "Elevation correction and building extraction from Interferometric SAR imagery," Proc. of *IGARSS'96*, Vol. I, pp. 659-661, Lincoln, Nebraska, July 1996.

[23] U. Weidner, "Building extraction from Digital Elevation Models," *Technical Report*, Institut fur Photogrammetrie, Bonn, 1995.

[24] R.W. Taylor, M. Savini, A.P. Reeves, "Fast segmentation of range imagery into planar regions", *Comput. Vision Graphics Image Processing*, Vol. 45, pp. 42-60, 1989.

[25] J. Mukherjee, P.P. Das, B.N. Chatterji, "Segmentation of range images," *Pattern Recognition*, Vol. 25, No. 10, pp. 1141-1156, 1992.

[26] X. Jiang and H. Bunke, "Fast segmentation of range images into planar regions by scan line grouping," *Machine Vision and Applications*, No. 7, pp. 115-122, 1994.

[27] R.O. Duda and P.E. Hart, *Pattern classification and scene analysis*, Wiley, New York, 1972.

[28] Y. Sheng and Z.-G. Xia, "A comprehensive evaluation of filters for radar speckle suppression," Proc. of *IGARSS'96*, Vol. II, pp. 1559-1561, Lincoln, Nebraska, July 1996.

[29] L. Alparone, B. Aiazzi, S. Baronti, C. Susini, Proc. of *IGARSS'96*, Vol. I, pp. 411-413, Lincoln, Nebraska, July 1996.

[30] C.H. Fosgate, H. Krim, W.W. Irving, W.C. Karl, A.S. Willsky, "Multiscale segmentation and anomaly enhancement of SAR images," *IEEE Trans. Image Proc.*, Vol. 6, No.1 , pp. 7-20, 1997.

[31] R.M. Goldstein, H.A. Zebker, C.L. Werner, "Satellite radar interferometry: two-dimensional phase unwrapping," *Radio Science*, Vol. 23 No. 4, pp. 713-720, 1988.

[32] Q. Lin, J.F. Vesecky, H.A Zebker., "New approaches in interferometric SAR data processing," *IEEE Trans. on Geoscience and Remote Sensing*, Vol. 30, No. 3, 1992.

Figure Captions

- Fig. 1: The block diagram of the segmentation algorithm used to analyze the IFSAR images.
- Fig. 2: On the right, an AIRSAR C-band image of Santa Monica, West Los Angeles (VV polarization). For a visual comparison, on the left an aerial photo of the same area is displayed. The blocks of black pixels correspond to large building shadows in the photograph, and to pixels labeled as "erroneous acquisition" in the SAR data.
- Fig. 3: Zoomed views of the aerial image in fig. 2 showing the three zones around Wilshire Boulevard that were analyzed in this paper.
- Fig. 4: The raw three-dimensional interferometric data provided by the TOPSAR system above the first zone of fig. 3 and the reconstructed building profiles after the data analysis.
- Fig. 5: The Coastal Federal Bank in Wilshire Boulevard: the building profile as reconstructed from IFSAR data and a photo from the ground.
- Fig. 6: 11755 Wilshire Boulevard: the building profile as reconstructed from IFSAR data and two photos from the ground.
- Fig. 7: The footprints of all the buildings extracted from the three subimages in fig. 3 compared with their actual sections (shadowed): a square corresponds to 25 mq.

TABLE I

PERCENTAGE ERROR IN DETERMINING THE BUILDING FOOTPRINTS BEFORE AND AFTER THE REFINEMENT STEP IN SECTION IV.A.

building	*before refinement*	*after refinement*
Coastal Federal Bank	-39%	-20%
World Savings	-48%	-25%
11755 Wilshire Boulevard	-67%	-37%
Barrington Plaza Apt.	-88%	-88%
11645 Wilshire Boulevard	-11%	-9%
L-shaped building	-50%	-1%

TABLE II

ACTUAL AND MEASURED HEIGHTS OF THE BUILDINGS EXTRACTED (MEAN ERROR = 2.2 M, σ = 4.9 M).

building	*actual height*	*measured height*	*absolute error*
Coastal Federal Bank	81	86	-5
World Savings	110	99	-11
11755 Wilshire Boulevard	98	99	+1
Barrington Plaza Apt.	74	71	-3
11645 Wilshire Boulevard	45	49	+4
L-shaped building	51	52	+1